

Magnitude and sign control of lithography-induced uniaxial anisotropy in ultra-thin (Ga,Mn)As wires

J. Shioyai,^{1,2,a)} D. Schuh,¹ W. Wegscheider,^{1,3} M. Kohda,^{2,4} J. Nitta,² and D. Weiss¹

¹Institute of Experimental and Applied Physics, University of Regensburg, 93053 Regensburg, Germany

²Department of Materials Science, Tohoku University, 980-8579 Sendai, Japan

³Department of Physics, ETH Zürich, 8093 Zürich, Switzerland

⁴PRESTO, Japan Science and Technology Agency, 332-0012 Kawaguchi, Japan

(Received 14 December 2010; accepted 25 January 2011; published online 22 February 2011)

We were able to control the magnitude and sign of the uniaxial anisotropy in 5-nm-thin (Ga,Mn)As wires by changing the crystallographic direction of the lithography-induced strain relaxation. The 1- μm -wide (Ga,Mn)As wires, oriented in $[110]$ and $[1\bar{1}0]$ directions, were fabricated using electron beam lithography. Their magnetic anisotropies were studied by a coherent rotation method at temperatures between 4.5 and 75 K. Depending on the orientation of the wire, the additional uniaxial anisotropy observed along the axis of the 1- μm -wide samples either increased or decreased the total uniaxial anisotropy. © 2011 American Institute of Physics. [doi:10.1063/1.3556556]

The electrical manipulation of the magnetization vector in ferromagnets is one of the most important areas of focus in spintronics. A material particularly well-suited to such investigations is the ferromagnetic semiconductor (Ga,Mn)As. (Ga,Mn)As exhibits hole-mediated ferromagnetism^{1,2} and its magnetic anisotropy depends on hole concentration, Mn concentration, lattice strain, and spin-orbit interaction.²⁻⁷ Recently, magnetization vector rotation by an electric field has been demonstrated in (Ga,Mn)As,⁸ and both experiments and simulations have shown that the modulation of the uniaxial anisotropy along $\langle 110 \rangle$ plays an important role in magnetization switching.⁹ One of the methods for controlling the uniaxial anisotropy is the modulation of the lattice strain in (Ga,Mn)As.⁴ Lithography-induced uniaxial anisotropy due to the magnetostriction effect has been observed in relatively thick (Ga,Mn)As wires on GaAs.¹⁰⁻¹⁵ Since the lithography-induced anisotropy can be externally modulated by changing the wire width¹⁵ after the crystal growth, it enables the switching of the magnetization of (Ga,Mn)As by an electric field with adjusted uniaxial anisotropy in combination with lithography-induced uniaxial anisotropies.

In this Letter, we prove the presence of the lithography-induced uniaxial anisotropy in 1- μm -wide ultrathin (Ga,Mn)As wires and also propose that this effect can assist in the electrical manipulation of magnetization.

Devices were fabricated from a single wafer consisting of 5-nm-thin (Ga_{0.94},Mn_{0.06})As grown on a semi-insulating GaAs substrate. Since the lattice constant of (Ga,Mn)As is larger than that of GaAs, a compressive strain is built into (Ga,Mn)As, which induces an in-plane magnetic easy axis. Its Curie temperature of 100 K was determined by a superconducting quantum interferometer device (SQUID). The wafer was patterned into 40- μm -long narrow wires with different wire widths, 1 and 20 μm , by electron beam lithography and reactive ion etching. We prepared two sets of 1- μm -wide wires oriented along either the $[110]$ or the $[1\bar{1}0]$ direction and a 20- μm -wide wire oriented along $[110]$. Figure 1 shows a scanning electron micrograph of the geometry of the final device. Magnetoresistance was probed by four-

point measurements at various temperatures between 4.5 and 75 K. External magnetic fields, $\mu_0 H_{\text{ex}} = 1.0$ and 0.1 T, were applied and rotated in-plane. The angle of the magnetic field φ_H was defined with respect to $[1\bar{1}0]$, as depicted in Fig. 1.

Figures 2(a) and 2(b) show the angular dependence of the anisotropic magnetoresistance (AMR) for the 20- μm -wide wire at $T = 4.5$ and 75 K for $\mu_0 H_{\text{ex}} = 1.0$ T. Figures 2(c) and 2(d) show the same type of data for the 1- μm -wide wires in $[110]$ (blue squares) and $[1\bar{1}0]$ (green circles) directions, respectively. Here, AMR is defined as $\text{AMR} = (R - R_{\text{min}}) / R_{\text{min}}$, where R is the longitudinal resistance of the wire and R_{min} is its minimal value. At $\mu_0 H_{\text{ex}} = 1.0$ T, the magnetization of (Ga,Mn)As is expected to be parallel to $\mu_0 H_{\text{ex}}$. In our case, the highest and lowest resistances correspond to the magnetization direction both parallel and perpendicular to the current direction, respectively. A similar behavior was observed in thinner (Ga,Mn)As.¹⁶ An expanded expression for the AMR was described by^{17,18}

$$\text{AMR} = -(C_I - C_{IC})\cos 2\varphi_M - C_C \cos 4\varphi_M, \quad (1)$$

for the 20- μm -wide wire along $[110]$, and

$$\text{AMR} = \mp (C_I - C_{IC} + C_U^{[110]/[1\bar{1}0]})\cos 2\varphi_M - C_C \cos 4\varphi_M + C_{IU}^{[110]/[1\bar{1}0]}, \quad (2)$$

for the 1- μm -wide wires along $[110]$ and $[1\bar{1}0]$ ($-$ for $[110]$ oriented wire and $+$ for $[1\bar{1}0]$ oriented wire). The angle of

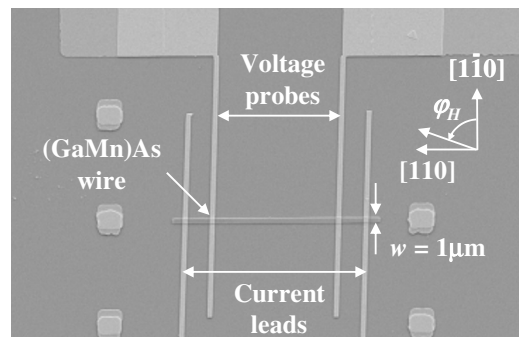


FIG. 1. SEM picture of 1- μm -wide (Ga,Mn)As wire device.

^{a)}Electronic mail: a9tm5316@cs.he.tohoku.ac.jp.

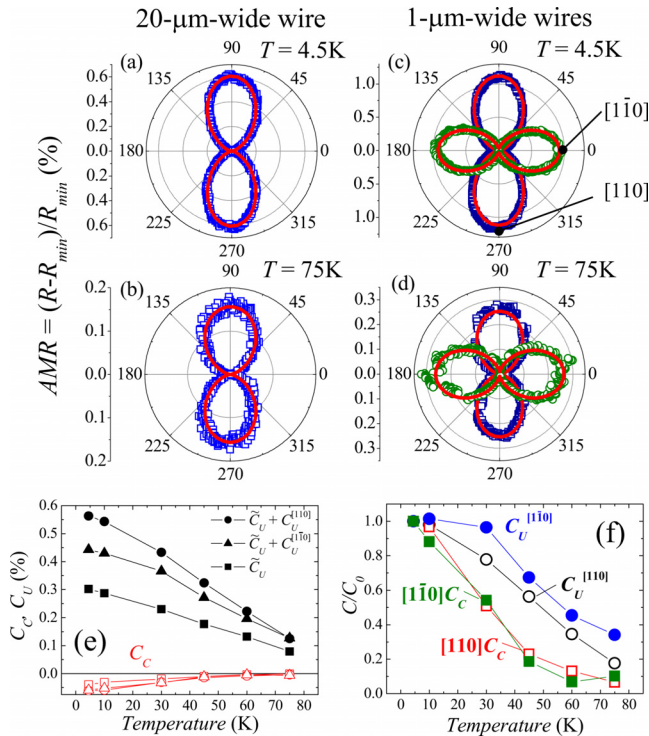


FIG. 2. (Color online) Angular dependences of the AMR at $\mu_0 H_{ex} = 1.0$ T for the 20- μm -wide wire at (a) 4.5 K and (b) 75 K, and the 1- μm -wide wires at (c) 4.5 K and (d) 75 K. In (c) and (d), the open squares are for the [110]-oriented wire and the open circles are for the $[1\bar{1}0]$ -oriented wire. (e) Temperature dependence of the AMR coefficients, the uniaxial term \tilde{C}_U , $C_U^{[110]/[1\bar{1}0]}$ and the cubic term C_C . Circles, triangles, and squares correspond to the 1- μm -wide wires along [110] and $[1\bar{1}0]$ direction, and the 20- μm -wide wire, respectively. The filled symbols are for either \tilde{C}_U or $\tilde{C}_U + C_U^{[110]/[1\bar{1}0]}$ and the open symbols are for C_C . (f) AMR coefficients normalized by the respective values of C_0 at 4.5 K for the 1- μm -wide wires. C_C is the cubic term and C_U is the additional uniaxial term. [110] and $[1\bar{1}0]$ correspond to the wire direction.

magnetization with respect to the $[1\bar{1}0]$ direction is denoted by ϕ_M . The values for C_I , C_{IC} , and C_C indicate the non-crystalline, the crossed non-crystalline/crystalline, and the cubic crystalline AMR coefficients, respectively.¹⁷ Both $C_U^{[110]/[1\bar{1}0]}$ and $C_U^{[110]/[1\bar{1}0]}$ stem from uniaxial distortion due to the lithography-induced strain relaxation. The AMR coefficients C_I , C_{IC} , C_C , $C_U^{[110]/[1\bar{1}0]}$, and $C_U^{[110]/[1\bar{1}0]}$ are obtained from Figs. 2(a)–2(d) by fitting with Eqs. (1) and (2). Figure 2(e) shows the temperature dependence of the magnitude of the uniaxial AMR coefficient $\tilde{C}_U = C_I - C_{IC}$, for the 20- μm -wide wire (filled squares), the sum of \tilde{C}_U and $C_U^{[110]/[1\bar{1}0]}$ for the 1- μm -wide wires (the filled circles and triangles), and the cubic crystalline AMR coefficient C_C (the open squares, circles, and triangles). In the whole temperature range, the uniaxial AMR coefficient [the first term in Eq. (2)] for the 1- μm -wide wires is by a factor of 1.5- μm -wide 20- μm -wide wire [the first term in Eq. (1)]. This can be attributed to the additional $C_U^{[110]/[1\bar{1}0]}$ of the uniaxial AMR coefficient in Eq. (2), which, in turn, can be attributed to the contribution made by the sizeable patterning-induced strain relaxation. Figure 2(f) summarizes the values of $C_U^{[110]/[1\bar{1}0]}$ and C_C for the 1- μm -wide wires at different wire directions normalized with respect to the corresponding coefficients C_0

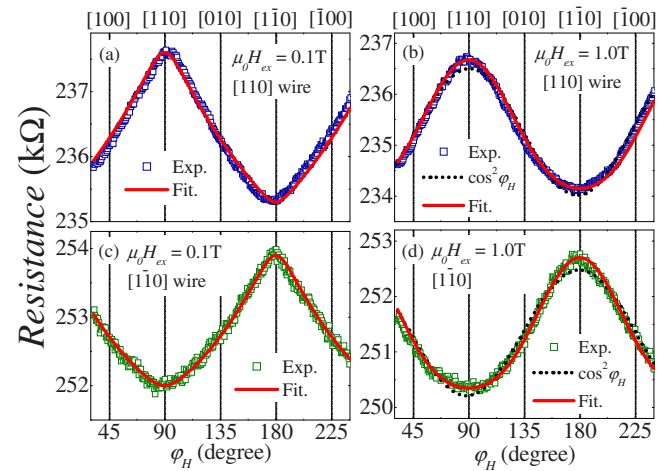


FIG. 3. (Color online) Angular dependences of the AMR for the 1- μm -wide (Ga,Mn)As wires at 4.5 K. (a) Wire direction along [110] and $\mu_0 H_{ex} = 0.1$ T. (b) Wire direction along [110] and $\mu_0 H_{ex} = 1.0$ T. (c) Wire direction along $[1\bar{1}0]$ and $\mu_0 H_{ex} = 0.1$ T. (d) Wire direction is along $[1\bar{1}0]$ and $\mu_0 H_{ex} = 1.0$ T, respectively.

at 4.5 K. The cubic terms, [110] C_C and $[1\bar{1}0]$ C_C , decrease more rapidly than $C_U^{[110]/[1\bar{1}0]}$ with increasing temperature, as C_C and $C_U^{[110]/[1\bar{1}0]}$ correlate with the cubic and the uniaxial magnetic anisotropies of (Ga,Mn)As, respectively.^{17,18}

Figures 3(a)–3(d) show the angular dependences of the AMR results for 1- μm -wide wires oriented along the [110] and $[1\bar{1}0]$ at 4.5 K for both $\mu_0 H_{ex} = 0.1$ and 1.0 T. Here, ϕ_H is the angle of $\mu_0 \mathbf{H}_{ex}$ with respect to the $[1\bar{1}0]$ direction. While $\mu_0 H_{ex} = 1.0$ T is strong enough for the (Ga,Mn)As magnetization to be parallel to $\mu_0 \mathbf{H}_{ex}$, the results in Figs. 3(b) and 3(d) deviate from the usual $\cos^2 \phi_H$ dependence because of the four-fold crystallographic term C_C in Eq. (2). The black dotted and red solid lines are the best fit results using $\cos^2 \phi_H$ and Eq. (2), respectively, which clearly indicate that the Eq. (2) shows a better fitting with the experimental data. The distorted shape is unchanged even for $\mu_0 H_{ex} = 10$ T (not shown). We referred to the difference in the traces measured at 0.1 and 1.0 T to determine the uniaxial anisotropy. The AMR measured at $\mu_0 H_{ex} = 0.1$ T [Figs. 3(a) and 3(c)], differs notably from the curve at $\mu_0 H_{ex} = 1.0$ T [Figs. 3(b) and 3(d)], and this was observed for both wire directions. At 1 T, the magnetization essentially follows the external magnetic field direction, while at 0.1 T the uniaxial anisotropy, along either [110] or $[1\bar{1}0]$ direction, impedes magnetization rotation. In order to evaluate the magnetic anisotropy constants, a coherent rotation model was employed.^{8,19–21} The total magnetic energy density is given by

$$E_{\text{mag}} = \frac{K_C}{4} \sin^2 2(\phi_M - 45^\circ) + K_U \sin^2 \phi_M - HM \cos(\phi_M - \phi_H), \quad (3)$$

where K_C and K_U are the cubic and the total uniaxial anisotropy constants, and H and M are the strength of external magnetic field and the saturation magnetization, respectively. From SQUID measurements, M was determined to be 35 mT at 4.5 K. The first term corresponds to the cubic anisotropy energy along $\langle 100 \rangle$, the second term to the uniaxial anisotropy along $[1\bar{1}0]$, and the third term to the Zeeman energy.

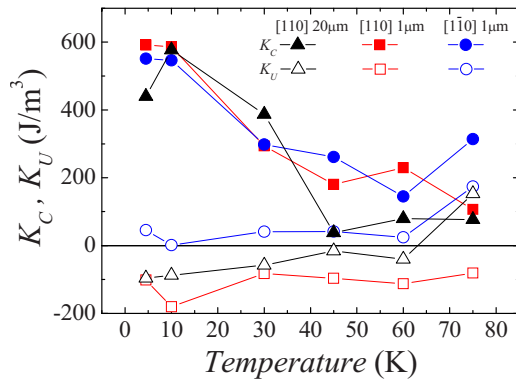


FIG. 4. (Color online) Temperature dependence of the magnetic anisotropy constants K_C and K_U obtained from the 20- μm -wide wire and the 1- μm -wide wires along $[110]$ and $[1\bar{1}0]$ directions.

To extract φ_M , the angular dependence of the AMR is fitted by minimizing E_{mag} ($\partial E_{\text{mag}}/\partial\varphi_M=0$ and $\partial^2 E_{\text{mag}}/\partial\varphi_M^2>0$) with K_C and K_U as fitting parameters using a least-square technique and the extracted φ_M is subsequently substituted into Eq. (2). As can be seen in Figs. 3(a) and 3(c), all the experimental results are well fitted by Eq. (2) as solid lines. From fitting of Eqs. (2) and (3), we obtained $K_C=591\text{ J/m}^3$ and $K_U=-101\text{ J/m}^3$ for the $[110]$ -oriented wire and $K_C=551\text{ J/m}^3$ and $K_U=+45\text{ J/m}^3$ for the $[1\bar{1}0]$ -oriented wire at 4.5 K.

Figure 4 summarizes the temperature dependence of the magnetic anisotropy constants for both the 1- μm -wide and the 20- μm -wide wires. While K_C shows a similar dependence for all wires in the investigated temperature range, the magnitude of K_U for the 1- μm -wide wires increases more in the $[110]$ -oriented wire and decreases more in the $[1\bar{1}0]$ -oriented wire than it does in the 20- μm -wide wire. In addition, the temperature dependence of K_U is less sensitive than that of K_C . Since the strain relaxation is insensitive to temperature change, this also indicates that the additional contribution to K_U in the 1- μm -wide wires originates from the magnetostriction effect.

Then, the total uniaxial anisotropy constant can be rewritten as¹⁹

$$K_U^{[110]/[1\bar{1}0]} = K_U^{\text{int}} \pm \frac{3}{2}\lambda_{111}\sigma, \quad (4)$$

with K_U^{int} , the intrinsic uniaxial anisotropy constant, λ_{111} , the magnetostriction constant, and σ , the magnitude of stress, respectively. While the intrinsic uniaxial anisotropy K_U^{int} does not change, the contribution of magnetostriction changes its sign depending on the wire direction. That is the direction of the strain relaxation is rotated by 90° when the wire direction is changed from the $[110]$ to $[1\bar{1}0]$ direction. We obtained a K_U of -96.3 J/m^3 when fitting the 20- μm -wide wire at 4.5 K. In this case, the second term in Eq. (4) is absent and K_U is equal to K_U^{int} . If one assumes that the magnitude of $\lambda_{111}\sigma$ does not depend on the wire direction, the averaged value of $\lambda_{111}\sigma$ obtained by fitting the data of the 1- μm -wide wires (in $[110]$ and $[1\bar{1}0]$) at 4.5 K is -49.1 J/m^3 . This reveals that the strain-induced anisotropy is comparable to the intrinsic uniaxial anisotropy in (Ga,Mn)As and adds either a positive

or negative contribution to the intrinsic uniaxial anisotropy depending on the wire orientation, and this results in a change in the sign of the total uniaxial anisotropy constant.

In conclusion, we investigated the magnetic anisotropies in 1- μm -wide, ultra-thin (Ga,Mn)As wires oriented along $[110]$ and $[1\bar{1}0]$ crystallographic directions and found an additional uniaxial anisotropy, which tends to align along the wire direction. Since the lithography-induced anisotropy is fully extrinsic and its magnitude is comparable to the intrinsic uniaxial anisotropy, this anisotropy adds to the electrically tunable intrinsic uniaxial anisotropy, thus, assisting with the electrical-field induced magnetization switching.

This work was partly supported by German Science Foundation (DFG) via SFB 689, the Japan–Germany Strategic International Cooperative Program (Joint Research Type) from JST, and Grants-in-Aid from JSPS, MEXT. The authors thank D. Chiba for useful discussion.

¹H. Ohno, *Science* **281**, 951 (1998).

²T. Dietl, H. Ohno, F. Matsukura, J. Cibert, and D. Ferrand, *Science* **287**, 1019 (2000).

³M. Abolfath, T. Jungwirth, J. Brum, and A. H. MacDonald, *Phys. Rev. B* **63**, 054418 (2001).

⁴T. Dietl, H. Ohno, and F. Matsukura, *Phys. Rev. B* **63**, 195205 (2001).

⁵M. Sawicki, K.-Y. Wang, K. W. Edmonds, R. P. Campion, C. R. Staddon, N. R. S. Farley, C. T. Foxon, E. Papis, E. Kaminska, A. Piotrowska, T. Dietl, and B. L. Gallagher, *Phys. Rev. B* **71**, 121302(R) (2005).

⁶K. Hamaya, T. Watanabe, T. Taniyama, A. Oiwa, Y. Kitamoto, and Y. Yamazaki, *Phys. Rev. B* **74**, 045201 (2006).

⁷M. Sawicki, F. Matsukura, A. Idziaszek, T. Dietl, G. M. Schott, C. Rueter, C. Gould, G. Karczewski, G. Schmidt, and L. W. Molenkamp, *Phys. Rev. B* **70**, 245325 (2004).

⁸D. Chiba, M. Sawicki, Y. Nishitani, Y. Nakatani, F. Matsukura, and H. Ohno, *Nature (London)* **455**, 515 (2008).

⁹D. Chiba, Y. Nishitani, F. Matsukura, and H. Ohno, *Appl. Phys. Lett.* **96**, 192506 (2010).

¹⁰J. Wenisch, C. Gould, L. Ebel, J. Storz, K. Pappert, M. J. Schmidt, C. Kumpf, G. Schmidt, K. Brunner, and L. W. Molenkamp, *Phys. Rev. Lett.* **99**, 077201 (2007).

¹¹K. Hamaya, R. Moriya, A. Oiwa, T. Taniyama, Y. Kitamoto, and H. Munekata, *IEEE Trans. Magn.* **39**, 2785 (2003).

¹²S. C. Masmanidis, H. X. Tang, E. B. Myers, M. Li, K. De Greve, G. Vermeulen, W. Van Roy, and M. L. Roukes, *Phys. Rev. Lett.* **95**, 187206 (2005).

¹³S. Hümpfner, K. Pappert, J. Wenisch, K. Brunner, C. Gould, G. Schmidt, L. W. Molenkamp, M. Sawicki, and T. Dietl, *Appl. Phys. Lett.* **90**, 102102 (2007).

¹⁴K. Pappert, S. Hümpfner, C. Gould, J. Wenisch, K. Brunner, G. Schmidt, and L. W. Molenkamp, *Nat. Phys.* **3**, 573 (2007).

¹⁵M. Kohda, J. Ogawa, J. Shioyai, F. Matsukura, Y. Ohno, H. Ohno, and J. Nitta, *Physica E (Amsterdam)* **42**, 2685 (2010).

¹⁶A. W. Rushforth, A. D. Giddings, K. W. Edmonds, R. P. Campion, C. T. Foxon, and B. L. Gallagher, *Phys. Status Solidi C* **3**, 4078 (2006).

¹⁷E. De Ranieri, A. W. Rushforth, K. Vyborny, U. Rana, E. Ahmad, R. P. Campion, C. T. Foxon, B. L. Gallagher, A. C. Irvine, J. Wunderlich, and T. Jungwirth, *New J. Phys.* **10**, 065003 (2008).

¹⁸A. W. Rushforth, K. Vyborny, C. S. King, K. W. Edmonds, R. P. Campion, C. T. Foxon, J. Wunderlich, A. C. Irvine, P. Vasek, V. Novak, K. Olejnik, J. Sinova, T. Jungwirth, and B. L. Gallagher, *Phys. Rev. Lett.* **99**, 147207 (2007).

¹⁹S. Chikazumi, *Physics of Ferromagnetism* (Oxford University Press, New York, 1997).

²⁰H. X. Tang, R. K. Kawakami, D. D. Awschalom, and M. L. Roukes, *Phys. Rev. Lett.* **90**, 107201 (2003).

²¹T. Yamada, D. Chiba, F. Matsukura, S. Yakata, and H. Ohno, *Phys. Status Solidi C* **3**, 4086 (2006).